

A Scalable and Automated Recurrence Plot Method for Detecting Climate Change: The Case of the UTCI Bioclimatic Index in Central Europe

Monika Okoniewska¹, Piotr Sionkowski¹, Natalia Kruszewska¹, Krzysztof Błażejczyk, and Krzysztof Domino¹

Abstract—Recent decades have brought increasing effects of climate change and variation. Climate changes, indicated by various bioclimatic indices, influence the functioning of living organisms, including humans. Previous studies have documented multiyear fluctuations in such indices. In this study, we employ the Universal Thermal Climate Index (UTCI), a recently developed bioclimatic indicator designed to condense complex thermodynamic and meteorological conditions into a single value representing specific categories of thermal stress. The average annual UTCI values for the period 1826–2021 in Kraków, Poland, increased at a rate of 0.27 °C per decade, with the most pronounced rise observed during the winter season, as documented in prior studies. However, when considering the more recent period of 1951–2023, the trend intensifies significantly, reaching 0.61 °C per decade, indicating a clear acceleration in bioclimatic warming. In the present study, we apply an automatic recurrence plot (RP) analysis method to investigate these changes in human bioclimate. We introduce a novel approach by automating RP interpretation with a genetic algorithm and statistical deterministic analysis, thereby providing readers with ready-to-use algorithms. The research focuses on a univariate time series of UTCI recorded from 1951 to 2023 in three locations in Poland—a key region of Central Europe where air masses from different parts of the continent interact. The main conclusion from the analyzed data is the identification of a date range (1980–1990), making a phase-transition-type passage between two periods that differ in statistical behaviors of UTCI. This bioclimatic change led to an increase in the frequency of very strong heat stress events and a decrease in the occurrence of very strong cold stress days. The RP analysis demonstrates that the data from 1990 differ most from data from the preceding period 1952–1965. This provides details of the findings reported in previous research regarding climate change in Poland. This discovery of a distinct transitional period marking a shift in the climatic regime in Poland, based on RP analysis, enriches existing knowledge on regional climate change with new empirical evidence.

Received 10 July 2025; accepted 6 August 2025. Date of publication 11 August 2025; date of current version 22 August 2025. (Corresponding author: Natalia Kruszewska.)

Monika Okoniewska is with the Faculty of Geographical Sciences, Kazimierz Wielki University, 85-033 Bydgoszcz, Poland.

Piotr Sionkowski and Krzysztof Domino are with the Institute of Theoretical and Applied Informatics, Polish Academy of Sciences, 44-100 Gliwice, Poland.

Natalia Kruszewska is with the Group of Modeling of Physicochemical Processes, Faculty of Chemical Technology and Engineering, Bydgoszcz University of Science and Technology, 85-796 Bydgoszcz, Poland (e-mail: nkruszewska@pbs.edu.pl).

Krzysztof Błażejczyk is with the Institute of Geography and Spatial Organization, Polish Academy of Sciences, 00-818 Warsaw, Poland.

This article has supplementary downloadable material available at <https://doi.org/10.1109/TGRS.2025.3597503>, provided by the authors.

Digital Object Identifier 10.1109/TGRS.2025.3597503

Index Terms—Artificial intelligence, changing point determination, climate change, recurrence plot (RP), time series analysis, Universal Thermal Climate Index (UTCI) bioclimatic index.

I. INTRODUCTION

C LIMATE change is a major concern in modern climatology as it is important to humanity, ecosystems, and the global economy [1]. Thus, the problem needs a highly interdisciplinary, holistic approach. The observed features of climate are strongly affected by the ongoing rise in temperature at both regional and global scales [2], [3], [4]. They can lead to extreme weather events such as floods, droughts, hurricanes, and heat waves. These phenomena may threaten human life by increasing the risk of disease, hunger, mass migration, and military conflicts [5]. Climate change also leads to environmental changes, which may negatively impact biodiversity, marine, and terrestrial ecosystems, and the life cycles of many species. This may consequently lead to the extinction of species and the loss of valuable ecosystems [6], [7]. Climate change may harm the economy through infrastructural damage, agricultural losses, job losses in sectors exposed to weather changes, and increased costs associated with adapting to new conditions [8]. Therefore, combating climate change is becoming increasingly urgent and requires international cooperation, local action, and technological innovation to reduce greenhouse gas emissions and adapt to changes already occurring.

A range of studies has identified the early 1980s as a period of accelerated temperature shifts, resulting from a combination of anthropogenic forcing (mainly increased greenhouse gas concentrations) and natural factors, such as changes in large-scale atmospheric circulation and volcanic activity (e.g., the 1982 El Chichón eruption [9], [10]). This period also marks the onset of more rapid lake warming, driven by rising air temperatures, reduced ice cover duration, decreased cloudiness, and enhanced solar radiation, all contributing to stronger thermal stratification and elevated surface-water temperatures. These processes reflect broader climate dynamics and underscore the role of lakes as sensitive indicators of both anthropogenic and natural climate variability [11].

The Intergovernmental Panel on Climate Change (IPCC) reports demonstrate the scale and possible causes of observed global and regional climate changes [12], [13]. There are several studies on climate change in Europe based on observational data [3], [14]. In Central Europe (Poland in particular), there are well-documented meteorological observation records

dating back to the early 19th century [15], [16], [17], [18]. Spatial analyses of climate change became feasible with the densification of meteorological measurement networks. In Poland, such analyses are possible for the period after 1950 [19].

In general, the strongest temperature increase is observed in the high-latitude regions of the Northern Hemisphere. In the zone north of parallel 64°N, the average increase is more than twice as high as globally [12]. This is due to several factors, including the presence of European land in the Arctic, which is the fastest warming region on Earth, and changes in atmospheric circulation that favor more frequent summer heatwaves. Therefore, climate change in Central Europe is not a regional phenomenon, but a part of and an indicator of global climate change. It has potentially significant consequences for all of Europe, impacting environmental protection, economic stability, and social stability [1].

The progression of climate change influences the bioclimatic conditions of all living organisms, including humans. The analysis of bioclimatic conditions considers not only air temperature, but also solar radiation, air humidity, and wind speed. Changes in all of these elements impact bioclimatic indices. Due to the challenges in accessing long-term observations of the aforementioned climate elements, studies on long-term changes in bioclimatic conditions are scarce. A unique position in this field is held by studies on bioclimate changes in Kraków (Poland), based on monthly averages of climate elements covering the period since 1826 [20], [21]. Thus, recently, the new Universal Thermal Climate Index (UTCI) bioclimatic index has been introduced. Importantly, such an approach extracts meaningful multivariate climatic information into a single univariate UTCI index.

More detailed studies on bioclimate changes, based on daily values, cover shorter periods. Antonescu et al. [22] and Di Napoli et al. (2022) [23] studied periods of around 40 years. The longest daily series of bioclimatic condition changes in Poland was utilized by Owczarek [26] and Kuchcik et al. [24], [25]. These studies demonstrated a significant impact of bioclimate changes on climate-dependent mortality [27], [28].

Earlier research by Kuchcik [29] suggested biphasic changes in bioclimatic indices. At most stations in Poland, during the years 1975–1980, the rate, and sometimes the direction, of changes in bioclimatic indices shifted noticeably. The potential causes of this phenomenon remain an open question. Referring back to [21], the change point (CP) in the UTCI index dynamics was expected in 1941. This is in contrast with other research, e.g., [30], pointing out that the meaningful shift in the global climate occurred in the 1980s. Hereby, to assess potentially anthropological impact on climate change, we intend to develop a robust and cross-validated analytical approach to examine the actual changing point of the UTCI dynamics.

The study of changes and fluctuations in long-term climate data series requires the use of advanced analytical methods. Such analyses are often carried out through trend analysis, which involves assessing the direction of changes over a given period, such as increases or decreases in a particular

meteorological parameter or index [21], [31], [32]. This is done using a simple linear regression analysis method that helps evaluate the general direction of changes in data. Another approach is the use of statistical tests (e.g., the Mann–Kendall test), which are used to evaluate whether there is a statistically significant trend in a given time series [14], [17]; such an approach can be supported also by the application of Sen's Slope Estimator (also known as the Theil–Sen estimator) [33]. In cases where the changes in the data are nonlinear, nonlinear regression can also be applied. Another method is variability analysis, which helps assess whether the fluctuations in data are regular (e.g., seasonal) or chaotic. A key aspect of this analysis is the evaluation of whether changes in variability are related to other phenomena. A method used in variability analysis is the calculation of standard deviations [34], which is used to evaluate how far data deviate from the mean, potentially indicating changes in climate variability. Variance analysis is also used to understand whether variability over time is constant or changes depending on the period (e.g., seasonality). The study of cyclicity and seasonality can rely on the Fourier transform, which is used to detect cycles of differing frequencies in climate data [35], or on time series decomposition, which involves separating the data into components: trend, seasonality, and residuals. This enables the extraction of seasonal patterns and long-term changes. Another way to analyze long-term climate data series is regression analysis and predictive models, which can be used to predict how individual climate factors will change in the future [31], [36]. For this purpose, both linear and nonlinear regression are employed to model the relationships between different climate variables. For large and complex datasets, ARIMA models (autoregressive integrated moving average) are used [37], and to model interdependencies between multiple climate variables over time, vector autoregression (VAR) models are applied. It is worth noting that studies of chaos and periodicity can be conducted using the recurrence plots (RPs) method, whose application to climate change research is not particularly popular. Typically used in physics and chaos theory, RPs are in this article adapted for UTCI data to detect climate change patterns, introducing a new dimension in time series climate analysis. Keeping in mind that RP analysis starts appearing in the meteorological data analysis [38], [39], their applications are parameter and expert-dependent. Henceforth, our high-level goal is to utilize a standardized, codified, and rigorous approach to RP analysis that eliminates possible bias and human error. On top of that, the proposed automatic RP assessments require less work from qualified subject matter experts (SMEs) and allow processing more plots simultaneously and under workforce constraints. In literature, the automatic analysis of RPs [40], [41] means the automatic determination of RP parameters. We, however, shift this frontier to the application of automated methods also to “read” and analyze RP images. The main objective of our research is to propose a methodology for the assessment of climate change that is scalable and applicable to any time series and location, making it a valuable analytical tool for climatology and other disciplines concerned with the dynamics of complex systems. Specifically, the study aims to verify the

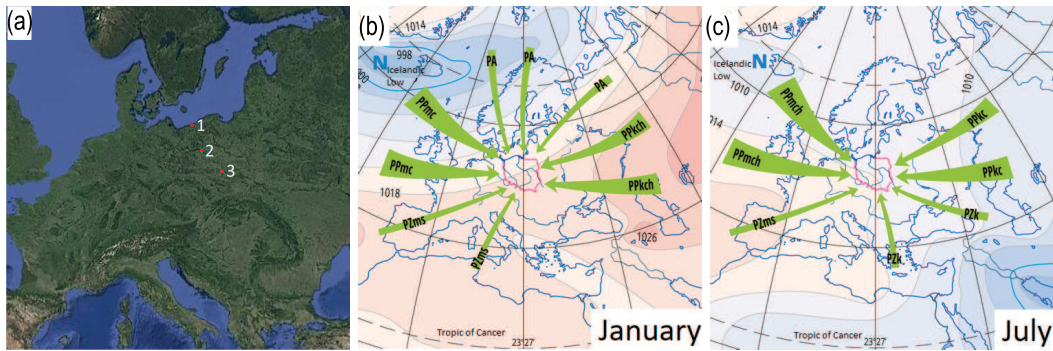


Fig. 1. (a) Map of Europe with the locations of the three measurement stations used to calculate UTCI: 1) Kołobrzeg represents the Southern Baltic Coastlands ($15^{\circ}34'E\ 54^{\circ}10'N$, hs 5 m a.s.l.); 2) Poznań is situated in the Poznań Lakeland ($16^{\circ}55'E\ 52^{\circ}25'N$, hs 86 m a.s.l.); and 3) Kraków is the main city of the Carpathian Foredeep ($19^{\circ}57'E\ 50^{\circ}03'N$, hs 220 m a.s.l.). Typical distribution of pressure systems in the European region and the air masses flowing into Poland. (b) January and (c) July [42]. Description of codes: PA-Arctic air masses, PP-polar air masses, PZ-tropical air masses, ch-cool air, c-warm air, m-maritime air, k-continental air, and s-air that has lost its original properties.

applicability of the RP method to assess changes in bioclimatic conditions, expressed through the multivariable and complex UTCI, utilizing Central Europe as a case study.

The research is based on previous analyses of multiannual variations in biothermal conditions, recorded at 12:00 UTC from 1951 to 2020 at three weather stations—Kołobrzeg, Poznań, and Kraków [32]. These prior analyses, based on the UTCI, are expanded in this article through the application of advanced statistical methods, including RPs and CP detection. A method for the automated reading of RPs is also proposed to enhance the objectivity and reproducibility of their interpretation. The study also examines CPs to identify shifts in biothermal conditions over the 70-year period and seeks to determine whether UTCI changes vary geographically along a north–south transect.

The particular objectives of the current study are as follows: 1) to analyze long-term changes in bioclimatic conditions in selected locations in Poland, a key European region where large air masses from different parts of the continent converge [see Fig. 1(a)]; 2) to verify whether the biphasic cycle of contemporary bioclimatic condition changes suggested by the aforementioned author will be confirmed over a period longer than that studied by Kuchcik; 3) to discuss the possible causes of this phenomenon; and 4) to verify whether the RP method can be applied in cases of climate and bioclimate long time series data to identify regional peculiarities of climate change.

As already mentioned, to measure bioclimatic conditions, we applied the UTCI index. To depict temporal and spatial variations, our analysis encompassed cities spanning a north–south transect [see Fig. 1(a)]. The study spanned from 1951 to 2023, focusing on the midday hours (12:00 UTC) frame to correlate the examined variations with the period when people typically engage in outdoor activities. Additionally, the study included an examination of CPs, pinpointing shifts in biothermal conditions over the 73 years under study.

II. MODEL AND METHOD

A. Studied Area

Poland is located in Central Europe, with a moderately warm climate that transitions between a maritime climate

in the western part and a continental climate in the eastern part [43]. We expect such an intermediate climate to be a good use case for our methodology, as phase-transition-like behavior (between marine climate and land climate dynamics) is expected here. The climate of Central Europe is shaped by as follows: 1) its location in the temperate zone of the northern hemisphere with prevailing westerly air currents and active cyclonic activity; 2) its being surrounded on three sides (to the north, west, and south) by seas and oceans and to the east by direct communication with the great landmass of Asia; 3) the predominance of east–west-oriented mountain chains; 4) the impact of the warm Gulf Stream. Climatic conditions are determined by the distribution of permanent or seasonal high- and low-pressure centers (high and low pressure). The main air-pressure centers influencing the climate of Europe, including Poland, are the Azores High and the Icelandic Low. In addition, the high-pressure center developing in Asia in winter and the continental low-pressure system in summer have a major impact. The Arctic High has a significant influence on the Arctic region. Three basic air masses flow over Central Europe: polar, Arctic, and tropical [see Fig. 1(b) and (c)]. These air masses are key factors contributing to the climatic diversity of Poland. Most often, the polar maritime air mass flows over the country (64.6%). The maritime air comes from the west, from the Atlantic Ocean, and brings warming in winter and cooling in summer. Polar continental masses bring dry and frosty weather in the winter, but in summer, they cause hot and sunny weather. From the north, there is advection of Arctic air masses (3.7%), which flows mainly in winter, bringing a drop in temperature and an increase in snowfall. Tropical air masses from the south flow over this part of Europe relatively rarely (2.0%). These are masses coming from the Azores islands or the Mediterranean Sea, so they are moist and very warm. In winter, their advection causes rapid warming, thaws, fogs, and drizzles, and, in summer, it causes heat waves. For about 230 days per year, atmospheric fronts cover Poland—most often cold fronts and, less often, warm fronts. A characteristic feature of this area of Europe is the direct proximity of periods without fronts to periods with the maximum frequency of atmospheric fronts.

TABLE I
RESPECTIVE VALUES OF UTCI CORRESPOND TO DIFFERENT CATEGORIES OF THERMAL STRESS

UTCI ($^{\circ}\text{C}$)	Stress category and recommendations for protection
> 46	extreme heat stress, periodical cooling and drinking $> 0.5\text{l}/\text{h}$ necessary; remain inactive
(38, 46]	very strong heat stress, periodical use of air conditioning or shaded sites, and drinking $> 0.5\text{l}/\text{h}$ necessary; reduce activity
(32, 38]	strong heat stress, drinking $> 0.25\text{l}/\text{h}$ necessary; use shaded places and reduce activity
(26, 32]	moderate heat stress, drinking $> 0.25\text{l}/\text{h}$ necessary
(9, 26]	no thermal stress, physiological thermoregulation sufficient to maintain comfort
(0, 9]	slight cold stress, use gloves and cap
(-13, 0]	moderate cold stress, increase activity, protect extremities and face against cooling
(-27, -13]	strong cold stress, strongly increase activity, protect face and extremities; use better-insulated clothing
(-40, -27]	very strong cold stress, strongly increase activity, protect face and extremities; use better-insulated clothing, reduce stay outdoor
< -40	extreme cold stress, stay indoors or use heavy, wind-protected clothing

B. Universal Thermal Climate Index

As already mentioned, the UTCI was applied as a measure of bioclimatic conditions. The UTCI has been used in many bioclimatic studies [22], [44], [45], [46], [47]. It is strongly dependent on air temperature [48], so it can also be useful for assessing climate change [21], [25]. The index provides complete information about thermophysiological processes in humans in the full range of possible environmental conditions (taking into account climate seasonality) and at all spatial scales [24], [49]. An important feature of the UTCI is its replacement of the multidimensional input and output information of the Fiala model with a 1-D value (expressed in degrees Celsius), which contains a similar load of information about physiological processes important from the point of view of the functioning of the human organism in changing ambient conditions. UTCI provides information on the actual processes of body temperature regulation, which depend on ambient meteorological conditions. Population characteristics, subjective individual characteristics, and the level of acclimatization do not play a significant role in shaping their level. In other words, the UTCI was developed based on the analysis of the human heat balance using the Fiala multinode heat transfer model. As a result, it enables the assessment of thermal comfort under various environmental conditions [50].

UTCI, as shown by Di Napoli et al. [51], can capture the thermal bioclimatic variability of Europe and link this variability with the impact it has on human health.

A multicomponent polynomial function, f , is used to calculate the UTCI index at the given (i 'th) timestamp

$$\text{UTCI}_i = T_a(i) + f(T_a(i), v_p(i), v_a(i), d_{Tmrt}(i)) \quad (1)$$

where variables are given as follows.

- 1) $T_a(i)$ is the air temperature ($^{\circ}\text{C}$) at timestamp i .
- 2) v_p is the water vapor pressure (hPa).
- 3) v_a is the wind speed at a height of 10 m above the ground (m s^{-1}).
- 4) d_{Tmrt} is the difference between the mean radiant temperature and air temperature ($^{\circ}\text{C}$).

and $i \in \{1, 2, \dots, N\}$. The regression function f is an offset function, which comprises 210 terms, as detailed in Annex 1 in Błażejczyk et al. [52]. The offset function takes into account all primary human physiological reactions to the thermal environment (such as vasomotor regulation, sweating, shivering, and changes in metabolic heat production). It is approximated

by a polynomial in $T_a(i)$, $v_p(i)$, $v_a(i)$, and $d_{Tmrt}(i)$ up to the 6th order. The approach used to determine the coefficients of the regression function is described in [53]. Due to the nonlinear integration of UTCI components, changes in its values may exhibit different dynamics than changes in the individual input parameters. For example, small variations in wind speed or humidity can lead to significant changes in perceived thermal comfort, which may not be proportional to changes in air temperature alone. In the context of climate change, analyzing only average air temperatures can lead to underestimating the impact of extreme events on human health and well-being. UTCI, by taking into account various factors, allows for a more comprehensive assessment of thermal risk and more accurate planning of adaptation measures, e.g., weather warnings, urban planning, or design of public spaces. In addition, indicators such as UTCI are important for medical services and crisis management institutions because they indicate better than temperature alone when health-threatening conditions occur, for example, for the elderly, children, or people with cardiovascular diseases. These considerations underscore the relevance of studying the dynamics of the change in UTCI. In this work, we propose an automated method for detecting and characterizing these dynamics. We aim to identify potential shifts or regime changes in the temporal behavior of the index.

The UTCI values were split into several categories of thermal stresses with specific recommendations for human behaviors under such conditions (see Table I). The UTCI is the index calculated on the basis of essential meteorological variables. Its range changes from about $-70\text{ }^{\circ}\text{C}$ to about $+50\text{ }^{\circ}\text{C}$. According to the research of [53], the root-mean-squared error (RMSE) of the predictions compared to the observed UTCI values for the grid data was $1.1\text{ }^{\circ}\text{C}$, with 50% of all errors falling within $\pm 0.6\text{ }^{\circ}\text{C}$, 80% within $\pm 1.3\text{ }^{\circ}\text{C}$, and 90% within $\pm 1.9\text{ }^{\circ}\text{C}$. In rare cases, extreme absolute deviations reached up to $6.2\text{ }^{\circ}\text{C}$.

C. Meteorological Input Data

The data used to compute UTCI were obtained from the Institute of Meteorology and Water Management (IMWM) database and comprise the following meteorological elements: air temperature ($^{\circ}\text{C}$), relative air humidity (%), wind speed ($\text{m} \cdot \text{s}^{-1}$), and cloud cover (oktas converted into %) [54]. All selected meteorological elements were measured at noon (12:00 UTC). The UTCI index was calculated using the

Algorithm 1 RP Computation

```

PREPROCESSING( $\vec{x}$ ) in our case  $\vec{x} = \text{UTCI}$ 
from time series  $\vec{x} = (x_1, x_2, \dots, x_N)$ ,
 $\vec{x}_{\tau}^{(1)} = (x_1, x_2, \dots, x_{N-\tau})$ 
 $\vec{x}_{\tau}^{(2)} = (x_{\tau+1}, x_{\tau+2}, \dots, x_{N-\tau})$ 
delay time  $\tau = \min\{\tau' : P(\text{cor}(\vec{x}_{\tau'}^{(1)}, \vec{x}_{\tau'}^{(2)}) = 0) > p\}$ 

$p = 0.05$  is significance level, see [68]

let  $\vec{y}_i^{(d,\tau)} = (x_i, x_{i+\tau}, x_{i+2\tau}, \dots, x_{i+d\tau})$ ,
 $\forall i$  compare  $\vec{y}_i^{(d,\tau)}$  and  $\vec{y}_i^{(d+1,\tau)}$  by Cao method [71]
find smallest  $d$  such that  $\vec{y}_i^{(d+1,\tau)}$  does not carry further
meaningful information compared with  $\vec{y}_i^{(d,\tau)}$  [71]
return  $\tau, d$ 

RECURRANCE PLOT( $\vec{x}, \tau, d, \lambda$ )
make  $m_{ii'}(\lambda) = \begin{cases} 0 & \text{if } \|\vec{y}_i^{(d,\tau)} - \vec{y}_{i'}^{(d,\tau)}\| \leq \lambda \\ 1 & \text{elsewhere} \end{cases}$ 
return visualize recurrent plot (white 0 dark 1)

```

BioKlima software (version 2.6) [55], which also processes IMWM data series to derive the parameters required for UTCI calculations [see (1)].

Data from three stations located in Poland were used for the analysis: Kołobrzeg, Poznań, and Kraków [see Fig. 1(a)]. Kołobrzeg represents the Southern Baltic Coastlands ($15^{\circ}\text{C}34'\text{E}$ $54^{\circ}\text{C}10'\text{N}$, 5 m a.s.l.) and is located on the Koszalin Coastland (Koszalin Coast mesoregion) [56]. The Kołobrzeg station is situated between the city and a health resort and is surrounded by dense, low-rise single-family buildings. The station was moved in 1971, but this did not affect the consistency of the measurement series. Poznań is located in the Poznań Lakeland ($16^{\circ}\text{C}55'\text{E}$ $52^{\circ}\text{C}25'\text{N}$, 86 m a.s.l.), which is part of the Central Poland Lowland [56]. The weather station is situated within the Poznań–Ławica airport on the city's western outskirts in a flat area free of natural and artificial obstructions. Kraków, the principal city of the Carpathian Foredeep ($19^{\circ}\text{C}57'\text{E}$ $50^{\circ}\text{C}03'\text{N}$, 220 m a.s.l.), is approximately 600 km from the Baltic Sea. The station is located in the Botanical Garden of the Jagiellonian University and was relocated in 1958, affecting the continuity of the wind series. However, analyses showed that this relocation did not significantly impact UTCI values.

D. RPs Approach

To extract meaningful information from UTCI time series within the analyzed geo-meteorological system, beyond CP analysis, we apply the RP approach [57]. The RP method is designed to reveal the behavior of complex (chaotic periodic) dynamical systems from time series data and to present this information graphically [58], [59]. This technique represents a novel approach to climate data analysis and has been applied only on a few occasions. The first studies to use RPs for climatic data were conducted on precipitation patterns in China [60] and periodic temperature variations in USA [61].

Technically, to construct an RP, from (1), we create the following vectors:

$$\vec{y}_i^{(d,\tau)} = (\text{UTCI}_i, \text{UTCI}_{i+\tau}, \text{UTCI}_{i+2\tau}, \dots, \text{UTCI}_{i+d\tau}) \quad (2)$$

where parameter τ is called the *delay time* and parameter d is called the *embedded dimension*. In this model, the dynamic of climate change is tied to the transformation $\vec{y}_i^{(d,\tau)} \rightarrow \vec{y}_{i'}^{(d,\tau)}$, where $i' > i$ and $i, i' \in \{1, 2, N - d\tau\}$. Then, the basic goal of the RP approach is to assess the dynamics of climate changes. The computation of RPs is presented in detail in Algorithm 1.

E. CP Analysis

To determine whether there is a specific time point (year) when bioclimatic conditions (based on UTCI) changed, the CP detection method was employed. CP analysis entails identifying moments within a dataset where there is a discernible shift in statistical properties. The Python package “ruptures” was used for this computation [62]. The CPs were counted using four different mathematical methods: Pruned Exact Linear Time (PELT) search [63], binary segmentation [64], window-based [65], and dynamic programming [66] methods. The PELT method is a penalized method, and it is not possible to define the number of changes to detect in advance. In the present study, a penalty value of 2 was chosen to avoid identifying too many CPs. The remaining three methods allow the number of changes to detect to be specified in advance, and this number was set to 1. Additionally, in each method, there is the possibility of choosing one of the following cost functions: kernelized mean change based on the radial basis function (rbf: detects changes in the mean of the embedded signal [67]), least absolute deviation (l1: detects changes in the median of a signal), or least squared deviation (l2: detects mean shifts in a signal).

III. RESULTS

This section is structured as follows. First, we create and analyze automatically the RPs to find the point of change in UTCI dynamics. Furthermore, we look for the CP to check whether common methods yield similar results. Finally, we perform trend analyses for data before and after the CP, to assess the significance of such a CP.

For RPs preparation, we apply the automatic parameter selection for RPs, using advanced methods (e.g., statistical testing and the Cao method) to automatically determine phase space reconstruction parameters (see [68], [69]), eliminate subjective bias, and enhance the reproducibility of the analysis. Then, we extend the automatic handling of RPs [40], [41] by introducing automatic methods for reading RPs, thus providing readers with ready-to-use algorithms.

The results of the RP analysis of the UTCI index are depicted in Fig. 2. On these plots, dark points yield the temporal coordinates i and i' [as in (2)] of data subseries that differ more than the given threshold value, and white points yield those subseries that differ less than the threshold value. Thus, dark regions represent intervals characterized by different dynamical behavior.

To this end, we first detect the series of years that differ most from all other data, namely the “dark crosses.” The dark crosses (enveloped by green lines) were detected using the statistical method introduced in [69] and presented here in Algorithm 2. Namely, the successive rows (or columns due

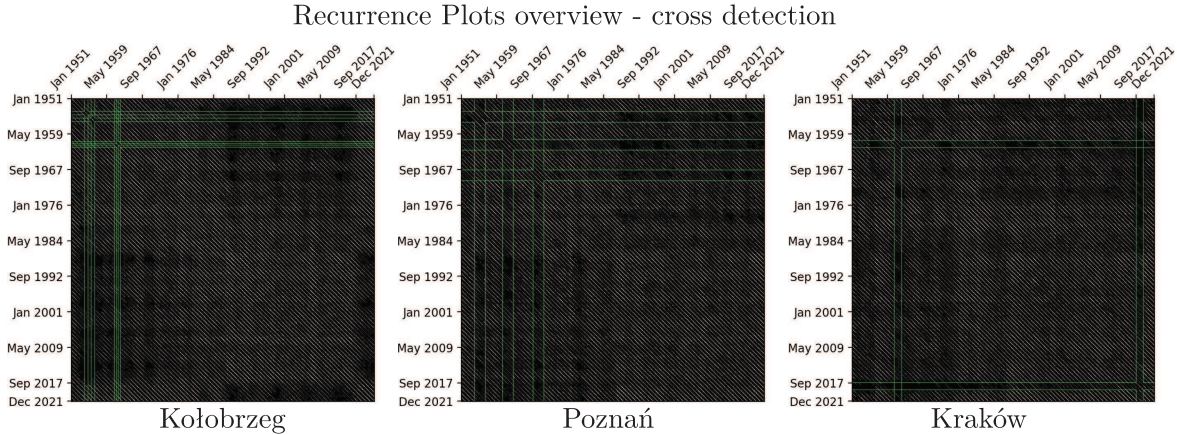


Fig. 2. RPs with dark crosses (global approach) detected by an algorithm introduced in [69]. Parameters of RPs: $\tau = 3$, $d = 8$ (automatically determined), and a recurrence rate (percentage of white points) of 9%, thresholds for cross detection (2σ). Note that most crosses are tied to the period before 1970, corresponding to particular dynamics in this time.

Algorithm 2 Cross Detection [69]

```
CROSS DETECT( $M$ ),  $M = [m_{i,i'}]$ ,  $m_{i,i'} = m_{i',i} \in \{0, 1\}$ 
let  $\vec{w} = w_i = \sum_{i'} m_{i,i'}$ 
for  $k \in \{k_{min} \dots k_{max}\}$ :
    let  $\vec{w}_{SMA_k}$  be  $\vec{w}$  smoothed with simple moving average of size  $k$ 
    let  $\vec{z}_k$  be standardized  $\vec{w}_{SMA_k}$  using z-score algorithm
end for
let  $k = \text{argmax}(\max(\vec{z}_k))$ 
let  $cc$  be local maxima of  $\vec{z}_k$  that are greater than threshold standard score
return cross centers  $cc$  and cross width  $k$ 
```

to symmetry) with the highest weight are marked as dark crosses. (The crosses in Fig. 2 show the observations that are most distant from all others.) From the graphical analysis (left and middle panels in particular), one can conclude that dark crosses appear before 1970, suggesting 1970 as the climate CP. In terms of the right panel, the information is less conclusive, as there is a dark cross around 2020. Thus, the more sophisticated methods of image analysis are necessary to assess climate change more rigorously.

For the assessment of automatic RPs, we propose a novel method that aims to detect dark squares that are of particular interest. Dark squares are regions that indicate the two sequences of years that differ most. Technically, our approach is presented in detail in Algorithms 3–5. The algorithms utilize genetic algorithms to find locally meaningful artifacts on the RPs. We use artificial intelligence to automatically detect visual patterns in RPs. Such an approach is rarely applied in biometeorology and represents an innovative fusion of AI and nonlinear dynamical system analysis.

Utilizing the results of such analysis, see dark squares in Fig. 3. (From the squares in Fig. 3, we see which data subseries are most distant in certain temporal ranges.) From dark squares, one can conclude that the subsequences that differ most from those in the years 1952–1965 are those in the 1990s. These two subsequences should lie on two different

Algorithm 3 Square Detection—Fitness Function

```
let square := ( $x, y, sidelen$ )
let  $M := [m_{i,i'}]$ ,  $m_{i,i'} = m_{i',i} \in \{0, 1\}$ 
FITNESS(square,  $w_{density}, w_{area}, M$ )
    let area = square.sidelen2
    return  $w_{density} \cdot \text{Density}(square, M) + w_{area} \cdot area$ 
DENSITY(square,  $M$ )
    let  $x = square.x$ 
    let  $y = square.y$ 
    let  $s = square.sidelen$ 
    let weight =  $\sum_{i=x}^{i=x+s} \sum_{i'=y}^{i'=y+s} m_{i,i'}$ 
    let area =  $s^2$ 
    return  $\frac{\text{weight}}{\text{area}}$ 
```

Algorithm 4 Square Detection—Offspring Creation

```
OFFSPRING( $square_1, square_2, d_{max} = 10$ )
    let  $\alpha = \text{random}(\text{Uniform}([0, 1]))$ 
    let  $x = \alpha \cdot square_1.x + (1 - \alpha) \cdot square_2.x$ 
    let  $y = \alpha \cdot square_1.y + (1 - \alpha) \cdot square_2.y$ 
    let  $\alpha = \text{random}(\text{Uniform}([0, 1]))$ 
    let  $s = \alpha \cdot square_1.sidelen + (1 - \alpha) \cdot square_2.sidelen$ 
     $x += \text{random}(\text{Uniform}([-d_{max}, d_{max}]))$ 
     $y += \text{random}(\text{Uniform}([-d_{max}, d_{max}]))$ 
    return  $(x, y, s)$ 
```

trends, split by the CP. Interestingly, dark squares lie on the dark crosses in Fig. 2, which validates our method.

To assess the robustness of the RPs, following [58], we estimate topological entropy, which measures the total complexity of the orbit structure of the chaotic system represented by the RP. The entropy values for subsequent RPs are as follows: Kołobrzeg: 3.3, Poznań: 3.4, and Kraków: 3.1. A Shannon entropy value of about 3, derived from an RP, could indicate a moderate level of complexity and unpredictability in the system's dynamics [70]. This suggests that while the system exhibits some irregular behavior, it does not display the high unpredictability characteristic of fully chaotic systems.

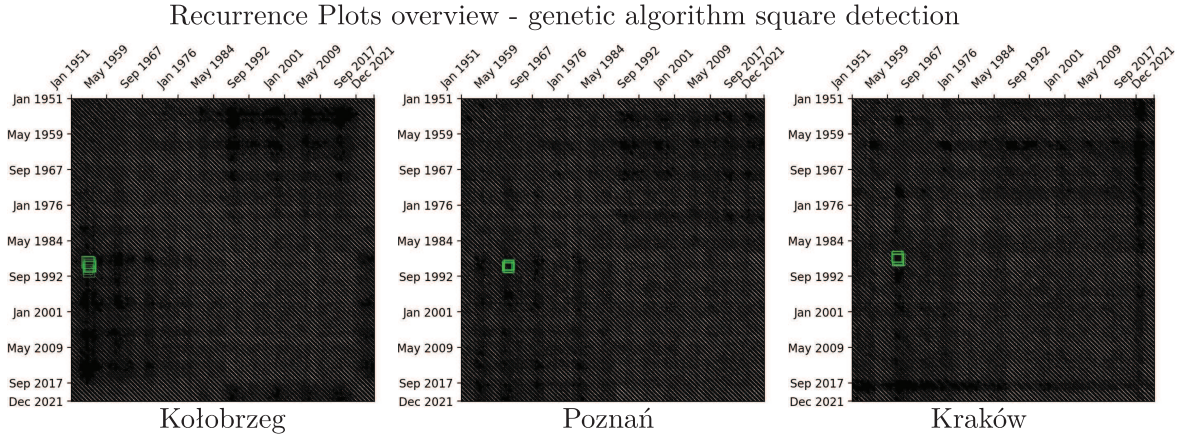


Fig. 3. RPs with dark squares (local approach) detected by genetic algorithm. Note that the detected square is stable in the y -coordinate but not in the x -coordinate. In other words, in all three plots, we found the date of the 1990s that most differs from those of the years 1952–1965.

Algorithm 5 Square Detection—Genetic Evolution

```

RANDOMSQUARE( $M, s_{min} = 30, s_{max} = 100$ )
let  $s = \text{random}(\text{Uniform}([s_{min}, s_{max}]))$ 
let  $x = \text{random}(\text{Uniform}([0, \text{len}(M) - s]))$ 
let  $y = \text{random}(\text{Uniform}([0, x]))$ 
return  $\text{square} = (x, y, s)$ 

GENETIC( $M, n_{gen}, n_{pop}$ ),  $n_{gen}, n_{pop} \in \mathbb{N}$ 
let  $\text{generation} = 0$ 
let  $\text{population} = \emptyset$ 
while #population <  $n_{pop}$ 
    population = population  $\cup$  RandomSquare( $M$ )
let  $\text{pop}_{fitness} = \text{sorted}(\text{population}, \text{Fitness})$ 
while  $\text{generation} < n_{gen}$ 
    //choose better half of the population as parents
    let  $\text{parents} = \text{first\_half}(\text{pop}_{fitness})$ 
    let  $\text{population} = \emptyset$ 
    while #population <  $n_{pop}$ 
        let  $p_1 = \text{chooseRandom}(\text{parents})$ 
        let  $p_2 = \text{chooseRandom}(\text{parents})$ 
        population = population  $\cup$  Offspring( $p_1, p_2$ )
    let  $\text{pop}_{fitness} = \text{sorted}(\text{population}, \text{Fitness})$ 
    generation = generation + 1
return best  $\text{pop}_{fitness}$ 

```

To validate the RP approach, we used state-of-the-art methods for CP detection in the UTCI time series for the three locations. First, to check whether the CPs are observed in every season, the calculations were made for UTCI monthly averaged data separately for each month of the year

$$\vec{\text{UTCI}} = (\text{UTCI}_1, \text{UTCI}_2, \dots, \text{UTCI}_{12}). \quad (3)$$

It is worth noting that a 73-year CP analysis of each month separately identified the same year (1981) as the point of change, indicating that the effect is not dependent on the season. An example of the analysis result for one month (May in Kraków) is shown in Fig. 4. It reveals a statistically significant increasing trend, as confirmed by the Mann–Kendall test ($\tau = 0.282$ and $p = 0.000417$), with a corresponding Sen’s slope of $0.639 \text{ }^{\circ}\text{C}/\text{decade}$. The trend in May is slightly greater than the

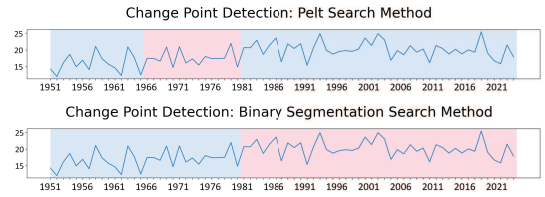


Fig. 4. Examples of CP analysis based on four CP methods (for may UTCI in Kraków, rbf). Regimes with different statistical behaviors are marked by alternating colors. Between them, CPs are estimated. The chart was obtained by the Python “ruptures” package. There is a statistically significant increasing trend (Mann–Kendall test: $\tau = 0.282$ and $p = 0.000417$), with a Sen’s slope of $0.639 \text{ }^{\circ}\text{C}/\text{decade}$.

overall annual trend for Kraków (slope = $0.608 \text{ }^{\circ}\text{C}/\text{decade}$); interestingly, the highest trend is observed in March (slope = $0.973 \text{ }^{\circ}\text{C}/\text{decade}$), while the lowest occurs in September (slope = $0.306 \text{ }^{\circ}\text{C}/\text{decade}$).

To assess climate change dynamics, we analyzed monthly UTCI time series from January 1951 to December 2023, resulting in three time series of $N = 876$ values each.

The analysis includes four CP detection methods, each employing three possible cost functions (see Section II-E). The results were then used to create histograms of detected CPs, from which the most frequently identified CPs could be discerned, see Fig. 5. Changing points mark the period of time when bioclimate conditions probably changed, suggesting a corresponding shift in the air-mass characteristics influencing the country’s climate. Based on the histograms in Fig. 5, the year 1981 is most frequently identified as the point at which a change in biothermal conditions occurred. The second such year is 1986, but the frequencies of attributing this year as the CP are considerably lower than those for 1981. This pattern recurs at all three stations. In Kraków, 1986 stands out as a year when some changes in biothermal conditions are also noticeable.

Example results obtained by Python’s “ruptures” package are depicted in Fig. 6. In the charts, a background color change indicates the identification of a CP. In this example, three methods identified 1981 as the CP, while one pointed to 1963. The Pelt method indicated only one CP; however, due



Fig. 5. Frequencies of the indication of the specific year as a CP by CP detection methods in Kolobrzeg, Poznań, and Kraków. Results have been split into three groups depending on the cost function used (I1-blue, I2-orange, and rbf-green). For example, number 3 inside the table above means that 3 of the four CP methods indicate this year as a CP.

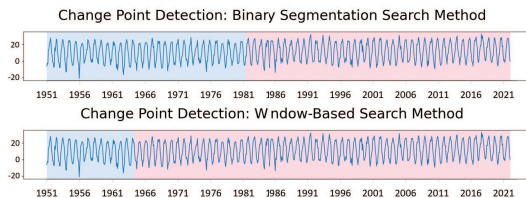


Fig. 6. Example results of CP analysis computed using the “ruptures” package for UTCI data for Kraków from January 1951 to December 2023 using the RBF cost function. There is a statistically significant increasing trend (Mann–Kendall test: $\tau = 0.0808$ and p-value = 0.00035), with a Sen’s slope of 0.608 °C/decade.

to the inability to specify the number of CPs to search for, this method often returned a large number of points, which affected the resulting histogram by adding CPs in the early years of the tested period. The remaining results of the CP analysis are available from the corresponding author upon request. Although all methods used for CP detection have limitations due to their dependence on the selected parameters, they confirm quantitative results obtained from RP analysis, i.e., namely, 1960s and 1990s are separated by the breaking point (see dark squares analysis), which most probably occurred after 1970 (see analysis of dark crosses).

Having identified the period in which the climate change occurred, it is essential to determine the direction and quantify the magnitude of these changes. We are performing these analyses to check whether our automatic RP-based algorithms point to a place where the meteorological trend is changed. To accomplish this, we analyzed UTCI yearly maximum and minimum values and calculated the regression lines before and after the identified phase-transition-type period (1980–1990), which is depicted in Fig. 7. A detailed analysis of regression lines for UTCI for the same measurement stations over a similar data range (1951–2020), treating all data as a single

TABLE II

RESULTS OF THE MANN–KENDALL TREND TEST AND SEN’S SLOPE (°C/decade) FOR ANNUAL MINIMUM AND MAXIMUM UTCI VALUES

Station	Variable	Period	τ	p-value	Sen’s slope
Kołobrzeg	min	<1980	0.297	0.0224	2.51
		>1990	-0.223	0.0868	-1.51
	max	<1980	0.159	0.225	0.704
		>1990	-0.108	0.412	-0.637
Poznań	min	<1980	0.122	0.354	1.44
		>1990	0.0575	0.669	0.608
	max	<1980	-0.113	0.392	-0.436
		>1990	-0.0345	0.803	-0.0724
Kraków	min	<1980	0.152	0.246	1.83
		>1990	0.0161	0.915	0.0908
	max	<1980	-0.0851	0.521	-0.333
		>1990	0.0897	0.498	0.214

time vector, is provided in [32]. Our research considers the dynamics before and after the 1980–1990 period, suggesting a phase-transition-type period. Specifically, in Kołobrzeg and Kraków from 1951 to 1980, minimum UTCI values remained consistently below the threshold of *very strong cold stress*. After the transitional period, from 1990 to 2020, these values shifted above this threshold, indicating a significant reduction in cold stress events. The case is similar for the maximum value in Kraków, where the shift to *above very strong heat stress* can be seen, suggesting in this case that more heat stress events appeared in recent years. Other cases also show an upward trend, approaching critical threshold values. In Kołobrzeg, there is a shift in trend from increasing to decreasing values, which is rather an unusual pattern, though previously documented for various cities and discussed in [19] and [25].

Another notable observation is that shifts in minimum UTCI values are considerably more pronounced than those in maximum UTCI values [32]. The average increase in UTCI is 6 °C–8 °C for minima and 1 °C–3 °C for maxima. The variance for minima exceeds 16.6 °C, whereas for maxima it remains below 8.5 °C.

We applied Student’s t-test to assess the statistical significance of differences in UTCI values before 1980 and after 1990. The test confirmed that the differences between these two periods were statistically significant. Subsequently, we applied the Mann–Kendall test to assess the presence of monotonic trends in the annual minimum and maximum UTCI values over time. We also analyzed the periods before 1980 and after 1990 separately. This analysis revealed weak trends, with only one result reaching statistical significance, while the others did not. Sen’s slope estimates indicated that the trends were of low order of magnitude, ranging approximately from 10 °C/decade to 10⁻² °C/decade. The results of this test are presented in Table II. Although most of the trends detected before 1980 were not statistically significant (with the exception of minimum UTCI in Kołobrzeg), they were generally stronger in magnitude compared to those observed after 1990. In the latter period, both the Mann–Kendall τ coefficients and Sen’s slope estimates were consistently lower, indicating weaker or negligible trends across all locations and variables. In conclusion, changes in trends before and after

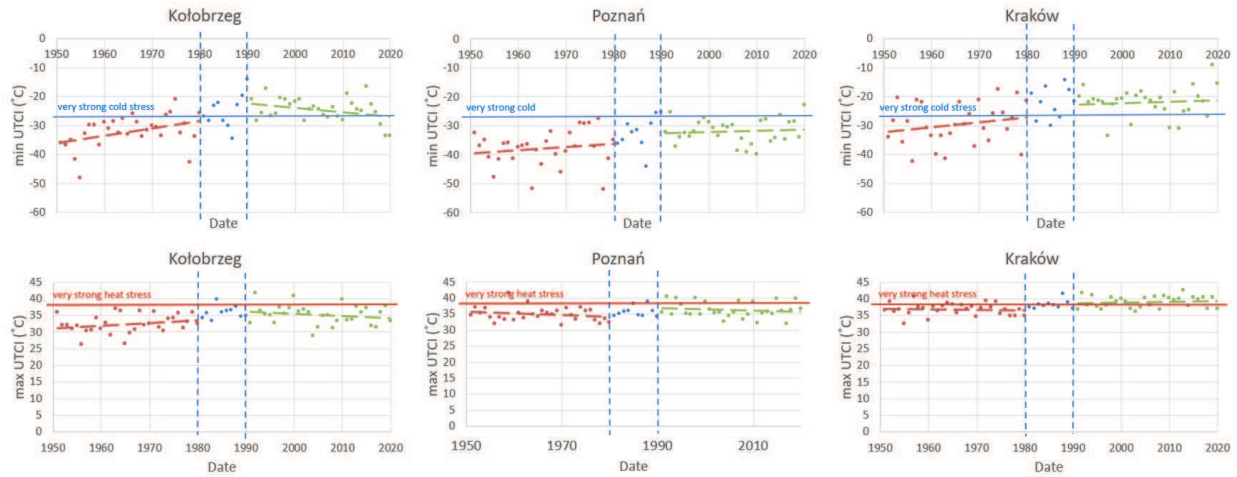


Fig. 7. Minimum and maximum UTCI at various locations. The time series is split by the 1980–1990 time window determined by various analytical methods as the transition period. Data behavior suggests a phase-transition-type passage in 1980–1990. The results of the trend analysis are presented in Table II.

the breaking point are weak but observable; importantly, such subtle differences in data dynamics have been assessed by the RP analysis.

IV. ALGORITHMS

In this section, we present particular algorithms for the RPs computation and automated analysis. RPs are computed according to the methodology applied in [69] for biomedical data analysis, as summarized in Algorithm 1. The time series is split into subseries using the statistical approach proposed in [68] and the Cao method [71] used as the state-of-the-art approach for this type of data. Each such subseries is assumed to carry meaningful (local in time) information on climate dynamics. The RP consists of white or dark dots, yielding whether the local subseries are similar or different (in terms of the vector norm). Henceforth, dark regions would yield different dynamics of two subseries tied to the time pinpointed on the x -axis and y -axis on the plot. The goal of subsequent algorithms is to determine such dark regions automatically.

To search for the global divergence of subseries, we use the cross-detection algorithm (Algorithm 2) introduced in [69]. On the RP, dark crosses represent the sequence of such subseries that most differ from all other data. Hence, we expect such dark crosses to be tied to the time range in which the climate dynamics were most unusual. In more detail, the cross-detection algorithm is based on the statistical analysis (and outlier detection) from the one-axis sum over the RP.

To search for the local divergence of subseries, in Algorithms 3–5, we introduce the author's in-house genetic approach for the detection of dark squares, which yields the most distinct subseries, one in range pinpointed on the x -axis and the other within a range pinpointed on the y -axis.

V. DISCUSSION AND CONCLUSION

Our motivation is to assess climate change on the example of Central Europe using standardized, codified, and rigorous approaches, hence potentially eliminating possible bias and

human error. With this, we aim to address a methodological gap in the search for the actual point of climate change, particularly concerning its impact on living organisms. This was achieved by employing the multisource UTCI index, which is an innovative approach, and by using advanced analytical approaches such as RP analysis supported by genetic algorithms.

It is worth noting that the use of artificial intelligence to automatically detect visual patterns in RPs remains rare not only in biometeorology but also across various other fields. This represents a novel integration of AI with nonlinear dynamical system analysis.

Following this, the automatic RP method indicates that climate change appears more as a phase-transition-type passage occurring between 1970 and 1990. This conclusion is based on the presence of dark crosses observed in the RP (see Fig. 2), particularly in the data before 1970, where cyclic subseries with unusual dynamics frequently appear. In contrast, the black squares (see Fig. 3), indicating the most statistically distinct measurement values, were identified by the genetic method between 1990 and the years 1952–1965. This phase-transition-type passage is not merely an observation based solely on temperature but instead reflects a shift in the mean and variance of an index based on multiple meteorological factors. This change has led to an increase in the frequency of very strong heat stress events and a decrease in the occurrence of very strong cold stress events. The average extrema values of UTCI show an increase of 6 °C–8 °C for minima and 1 °C–3 °C for maxima after the transition period. The method used in the current study to determine the CP in the trend line yielded similar results to the “hockey stick” method used by Kuchcik [29] in studying thermal and biothermal conditions in Poland at the turn of the 21st century.

The results show that the RP method can be used successfully in studies related to changes and fluctuations in climate and bioclimatic conditions. Hereby, our automated methods for analyzing UTCI change dynamics provide an objective framework for comparing climate-related thermal stress patterns across different regions of the world.

The key finding from the state-of-the-art CP analysis presented in Fig. 5 is that the year 1981 marks a division between two periods with distinct statistical patterns. This result is broadly consistent with the 2023 IMGW-PIB Report, which states that, until the mid-1980s, thermal conditions in individual years were typically classified as “cold” or “ool,” whereas from the second half of the 1980s onward, conditions increasingly fell into the categories of “normal” or “warmer” [72].

Similar findings are reported in a recent book on climate change in Poland [19]. The authors indicated that significant changes were observed in several climate elements during that period. Błażejczyk et al. [73] suggested that, in southern Poland (Kraków), such phenomena are related to changes in atmospheric circulation. This affects cloud cover and, consequently, the amount of incoming solar radiation [74].

Fluctuations in specific climate elements also influence changes in bioclimatic indicators [21], [24], [25], [73]. The combination of meteorological variables used to calculate bioclimatic indices, including the UTCI, makes the changes around 1980 more pronounced than those of individual variables [20].

ACKNOWLEDGMENT

This research is the result of cooperation within the BiOSS interdisciplinary group (<https://bioss-group.github.io/> accessed on 13 May 2025).

REFERENCES

- [1] H.-O. Pörtner et al., *Climate Change 2022—Impacts, Adaptation and Vulnerability: Working Group II Contribution To the Sixth Assessment Report of the Intergovernmental Panel on Climate Change*. Cambridge, U.K.: Cambridge Univ. Press, 2023.
- [2] T. Niedźwiedz, “Long-term variability of the zonal circulation index above the Central Europe,” in *Prace Geograficzne*, vol. 102. Warszawa, Poland: IGiPZ PAN, 1996, pp. 213–219.
- [3] R. Twardosz, A. Walanus, and I. Guzik, “Warming in Europe: Recent trends in annual and seasonal temperatures,” *Pure Appl. Geophys.*, vol. 178, no. 10, pp. 4021–4032, Oct. 2021.
- [4] U. Shahzad, “Global warming: Causes, effects and solutions,” *Durresam J.*, vol. 1, pp. 1–7, Aug. 2015.
- [5] K. D. Muslih and K. Błażejczyk, “Millennial and contemporary changes of middle east climate,” *Kosmos, Problemy Nauk Biologicznych*, vol. 70, no., vol. 4, no. 333, pp. 555–568, 2021.
- [6] S. Słowińska and M. Słowiński, “Torfowiska mszarne strefy północnej a zmiana klimatu (Northern peatlands and climate change),” *Kosmos, Problemy Nauk Biologicznych*, vol. 70, pp. 569–578, Jan. 2021.
- [7] A. Araźny, M. Kejna, T. Wawrzyniak, M. Osuch, J. Plenzler, and T. Budzik, “Zmiany klimatu w ekosystemach Arktyki i Antarktyki (climate change in the Arctic and Antarctic ecosystems),” *Kosmos, Problemy Nauk Biologicznych*, vol. 70, no. vol. pp. 579–595, 2021.
- [8] K. Abbass, M. Z. Qasim, H. Song, M. Murshed, H. Mahmood, and I. Younis, “A review of the global climate change impacts, adaptation, and sustainable mitigation measures,” *Environ. Sci. Pollut. Res.*, vol. 29, no. 28, pp. 42539–42559, Jun. 2022.
- [9] D. E. Parker and J. L. Brownscombe, “Stratospheric warming following the El Chichón volcanic eruption,” *Nature*, vol. 301, no. 5899, pp. 406–408, 1983.
- [10] R. S. Quiroz, “The isolation of stratospheric temperature change due to the el Chichón volcanic eruption from nonvolcanic signals,” *J. Geophys. Res., Oceans*, vol. 88, no. C11, pp. 6773–6780, Aug. 1983.
- [11] R. I. Woolway, M. T. Dokulil, W. Marszelewski, M. Schmid, D. Bouffard, and C. J. Merchant, “Warming of central European lakes and their response to the 1980s climate regime shift,” *Climatic Change*, vol. 142, nos. 3–4, pp. 505–520, Jun. 2017.
- [12] V. Masson-Delmotte et al., *Climate Change 2021: The Physical Science Basis. Contribution of Working Group I To the Sixth Assessment Report of the Intergovernmental Panel on Climate Change*. Cambridge, U.K.: Cambridge Univ. Press, 2021.
- [13] P. Arias et al., “Technical summary,” in *Climate Change 2021: The Physical Science Basis. Contribution of Working Group I to the Sixth Assessment Report of the Intergovernmental Panel on Climate Change*, V. Masson-Delmotte et al., Eds., Cambridge, U.K.: Cambridge Univ. Press, 2021, pp. 33–144.
- [14] B. Czernecki and M. Miętus, “The thermal seasons variability in Poland, 1951–2010,” *Theor. Appl. Climatol.*, vol. 127, nos. 1–2, pp. 481–493, Jan. 2017.
- [15] H. Lorenc, *Studio NAD 220-Letnią (1779-1998) Serią Temperatury Powietrza W Warszawie Oraz Ocena Jej Wiekowych Tendencji*(Materiały Badawcze Instytut Meteorologii i Gospodarki Wodnej: Meteorologia). San Diego, CA, USA: IMiGW, 2000.
- [16] K. Bryś and T. Bryś, “Reconstruction of the 217-year (1791–2007) Wrocław air temperature and precipitation series,” *Bull. Geography. Phys. Geography Ser.*, vol. 3, no. 1, pp. 121–171, Dec. 2010.
- [17] Z. Bielec-Bakowska and R. Twardosz, “Exceptionally cold and warm spring months in Kraków against the background of atmospheric circulation (1874–2022),” *Pure Appl. Geophys.*, vol. 180, no. 9, pp. 3351–3370, Sep. 2023.
- [18] J. Trepiska and L. Kowanetz, “Wieloletni przebieg średnich miesięcznych wartości temperatury powietrza w Krakowie (1792–1995),” in *Wahania Klimatu W Krakowie (1792–1995)*. Krakow, Poland: Instytut Geografii Uniwersytetu Jagiellońskiego, 1997.
- [19] M. Falarz, Ed., *Climate Change in Poland: Past, Present, Future (Springer Climate)*. Cham, Switzerland: Springer, 2021.
- [20] K. Błażejczyk and R. Twardosz, “Long-term changes of bioclimatic conditions in Cracow (Poland),” in *The Polish Climate in the European Context: An Historical Overview*. Dordrecht, The Netherlands: Springer, 2010, pp. 235–246.
- [21] K. Błażejczyk and R. Twardosz, “Secular changes (1826–2021) of human thermal stress according to UTCI in Kraków (Southern Poland),” *Int. J. Climatol.*, vol. 43, no. 9, pp. 4220–4230, Jul. 2023.
- [22] B. Antonescu et al., “A 41-year bioclimatology of thermal stress in Europe,” *Int. J. Climatol.*, vol. 41, no. 7, pp. 3934–3952, Jun. 2021.
- [23] C. Di Napoli, T. Allen, P. A. Méndez-Lázaro, and F. Pappenberger, “Heat stress in the caribbean: Climatology, drivers, and trends of human biometeorology indices,” *Int. J. Climatol.*, vol. 43, no. 1, pp. 405–425, Jan. 2023.
- [24] M. Kuchcik, K. Błażejczyk, and A. Halas, “Long-term changes in hazardous heat and cold stress in humans: Multi-city study in Poland,” *Int. J. Biometeorol.*, vol. 65, no. 9, pp. 1567–1578, Sep. 2021.
- [25] M. Kuchcik, K. Błażejczyk, and A. Halas, “Changes in bioclimatic indices,” in *Climate Change in Poland: Past, Present, Future*. Cham, Switzerland: Springer, 2021, pp. 471–491.
- [26] M. Owczarek, *Warunki Bioklimatyczne Na Wybrzeżu Pomorzu W Drugiej Poowie XX Wieku*(Materiały Badawcze-Instytut Meteorologii i Gospodarki Wodnej Pastwowy Instytut Badawczy, 2012).
- [27] A. Błażejczyk and J. Baranowski, “Wpływ zmian klimatu na zmiany zachorowań i zgonów na choroby klimatozależne w Polsce w XXI wieku,” *Kosmos*, vol. 70, no. 4, pp. 597–610, Feb. 2022. [Online]. Available: <https://api.semanticscholar.org/CorpusID:246507307>
- [28] M. Kuchcik, “Mortality and thermal environment (UTCI) in Poland—Long-term, multi-city study,” *Int. J. Biometeorol.*, vol. 65, no. 9, pp. 1529–1541, Sep. 2021.
- [29] M. Kuchcik, “Warunki termiczne w Polsce na przełomie XX i XXI wieku i ich wpływ na umieralność (Thermal conditions in Poland at the turn of the 20th and 21st centuries, and their impact on mortality),” in *Prace Geograficzne*. Warszawa, Poland: IGiPZ PAN, 2017.
- [30] P. C. Reid et al., “Global impacts of the 1980s regime shift,” *Global Change Biol.*, vol. 22, no. 2, pp. 682–703, Feb. 2016.
- [31] R. Mahmood, S. Jia, and W. Zhu, “Analysis of climate variability, trends, and prediction in the most active parts of the lake chad basin, Africa,” *Sci. Rep.*, vol. 9, no. 1, p. 6317, Apr. 2019.
- [32] M. Okoniewska, “Multi-annual variations in the heat load of Poland,” *Quæstiones Geographicæ*, vol. 43, no. 3, pp. 65–76, Sep. 2024.
- [33] B. F. Frimpong, A. Koranteng, and F. Molkenanthin, “Analysis of temperature variability utilising Mann–Kendall and Sen’s slope estimator tests in the Accra and Kumasi metropolises in Ghana,” *Environ. Syst. Res.*, vol. 11, no. 1, p. 24, Nov. 2022.
- [34] S. Robeson, “Relationships between mean and standard deviation of air temperature: Implications for global warming,” *Climate Res.*, vol. 22, no. 3, pp. 205–213, 2002.

- [35] K. Higuchi, J. Huang, and A. Shabbar, "A wavelet characterization of the North Atlantic oscillation variation and its relationship to the North Atlantic sea surface temperature," *Int. J. Climatol.*, vol. 19, no. 10, pp. 1119–1129, Aug. 1999.
- [36] T. B. M. J. Ouarda et al., "Prediction of heatwave related mortality magnitude, duration and frequency with climate variability and climate change information," *Stochastic Environ. Res. Risk Assessment*, vol. 38, no. 11, pp. 4471–4483, Nov. 2024.
- [37] S. Swain, S. Nandi, and P. Patel, "Development of an ARIMA model for monthly rainfall forecasting over khordha district, Odisha, India," in *Recent Findings in Intelligent Computing Techniques*. Singapore: Springer, 2018, pp. 325–331.
- [38] J. John Bejoy and G. Ambika, "Recurrence analysis of meteorological data from climate zones in India," *Chaos, Interdiscipl. J. Nonlinear Sci.*, vol. 34, no. 4, Apr. 2024, Art. no. 043150, doi: [10.1063/5.0165282](https://doi.org/10.1063/5.0165282).
- [39] Z. Q. Zhao, S. C. Li, J. B. Gao, and Y. L. Wang, "Identifying spatial patterns and dynamics of climate change using recurrence quantification analysis: A case study of Qinghai-Tibet Plateau," *Int. J. Bifurcation Chaos*, vol. 21, no. 4, pp. 1127–1139, Apr. 2011.
- [40] M. Jamrozy, K. Lewenstein, and T. Leyko, "Automatic analysis of recurrence plot for the needs of the analysis of infrasonic signals from the human heart," in *Mechatronics 2013: Recent Technological and Scientific Advances*. Cham, Switzerland: Springer, 2014, pp. 785–792.
- [41] R. Delage and T. Nakata, "An algorithm for simplified recurrence analysis," *Chaos, Interdiscipl. J. Nonlinear Sci.*, vol. 34, no. 9, Sep. 2024, Art. no. 093114, doi: [10.1063/5.0225465](https://doi.org/10.1063/5.0225465).
- [42] Serwis Ministerstwa Edukacji Narodowej.(2024). *Czynniki Kształtujące Klimat Polski*. [Online]. Available: <https://zpe.gov.pl/a/czynniki-ksztaltujace-klimat-polski/DblZrZd6v>
- [43] K. Błażejczyk, "Climate and bioclimate of Poland," in *Natural and Human Environment of Poland. A Geographical Overview*(Polish Academy of Sciences Institute of Geography and Spatial Organization). Warsaw, Poland: Polish Geographical Society, 2006, pp. 31–48.
- [44] A. Blesta, P. T. Nastos, and A. Matzarakis, "Assessment of bioclimatic conditions on Crete Island, Greece," *Regional Environ. Change*, vol. 14, no. 5, pp. 1967–1981, Oct. 2014.
- [45] R. Emerton et al., "Predicting the unprecedented: Forecasting the June 2021 Pacific Northwest heatwave," *Weather*, vol. 77, no. 8, pp. 272–279, Aug. 2022.
- [46] Y. Huang, D. Lai, Y. Liu, and X. Huang, "Impact of climate change on outdoor thermal comfort in cities in United States," *E3S Web Conf.*, vol. 158, Jan. 2020, Art. no. 01002.
- [47] M. Okoniewska, "Daily and seasonal variabilities of thermal stress (based on the UTCI) in air masses typical for central Europe: An example from Warsaw," *Int. J. Biometeorol.*, vol. 65, no. 9, pp. 1543–1552, Sep. 2021.
- [48] B. Kampmann, P. Bröde, and D. Fiala, "Physiological responses to temperature and humidity compared to the assessment by UTCI, WGBT and PHS," *Int. J. Biometeorol.*, vol. 56, no. 3, pp. 505–513, May 2012, doi: [10.1007/s00484-011-0410-0](https://doi.org/10.1007/s00484-011-0410-0).
- [49] G. Jendritzky, R. de Dear, and G. Havenith, "UTCI—Why another thermal index?," *Int. J. Biometeorol.*, vol. 56, no. 3, pp. 421–428, May 2012, doi: [10.1007/s00484-011-0513-7](https://doi.org/10.1007/s00484-011-0513-7).
- [50] J. Romaszko, E. Dragańska, R. Jalali, I. Cymes, and K. Glińska-Lewczuk, "Universal climate thermal index as a prognostic tool in medical science in the context of climate change: A systematic review," *Sci. Total Environ.*, vol. 828, Jul. 2022, Art. no. 154492.
- [51] C. Di Napoli, F. Pappenberger, and H. L. Cloke, "Assessing heat-related health risk in Europe via the universal thermal climate index (UTCI)," *Int. J. Biometeorol.*, vol. 62, no. 7, pp. 1155–1165, Jul. 2018.
- [52] K. Błażejczyk et al., "UTCI—nowy wskaźnik oceny obciążień cieplnych człowieka," *Przegląd Geograficzny*, vol. 82, no. 1, pp. 49–71, 2010.
- [53] P. Bröde et al., "Deriving the operational procedure for the universal thermal climate index (UTCI)," *Int. J. Biometeorol.*, vol. 56, no. 3, pp. 481–494, May 2012.
- [54] Instytut Meteorologii i Gospodarki Wodnej.(2024). *Dane Meteorologiczne*. [Online]. Available: https://danepubliczne.imgw.pl/data/dane_pomiarowo_oberwacyjne/
- [55] Institute of Geography and Spatial Organization, Polish Academy of Sciences.*Bioklima-Universal Tool for Bioclimatic and Thermo-physiological Studies*. Accessed: Nov. 6, 2024. [Online]. Available: <https://www.igipz.pan.pl/bioklima-crd.html>
- [56] J. Solon et al., "Physico-geographical mesoregions of Poland: Verification and adjustment of boundaries on the basis of contemporary spatial data," *Geographia Polonica*, vol. 91, no. 2, pp. 143–170, 2018.
- [57] B. Goswami, "A brief introduction to nonlinear time series analysis and recurrence plots," *Vibration*, vol. 2, no. 4, pp. 332–368, Dec. 2019.
- [58] N. Marwan, M. Carmenromano, M. Thiel, and J. Kurths, "Recurrence plots for the analysis of complex systems," *Phys. Rep.*, vol. 438, nos. 5–6, pp. 237–329, Jan. 2007.
- [59] M. Thiel, M. C. Romano, and J. Kurths, "How much information is contained in a recurrence plot?," *Phys. Lett. A*, vol. 330, no. 5, pp. 343–349, Sep. 2004.
- [60] W. Zhang, G. Feng, and Q. Liu, "The application of recurrence quantification analysis in detection of abrupt climate change," *Discrete Dyn. Nature Soc.*, vol. 2016, no. 1, pp. 1–7, 2016.
- [61] A. Bai, S. Hira, and S. D. Parag, "Recurrence based similarity identification of climate data," *Discrete Dyn. Nature Soc.*, vol. 2017, no. 1, pp. 1–21, 2017.
- [62] C. Truong, L. Oudre, and N. Vayatis, "Selective review of offline change point detection methods," *Signal Process.*, vol. 167, Feb. 2020, Art. no. 107299.
- [63] R. Killick, P. Fearnhead, and I. A. Eckley, "Optimal detection of changepoints with a linear computational cost," *J. Amer. Stat. Assoc.*, vol. 107, no. 500, pp. 1590–1598, Dec. 2012.
- [64] P. Fryzlewicz, "Wild binary segmentation for multiple change-point detection," *Ann. Statist.*, vol. 42, no. 6, pp. 2243–2281, Dec. 2014.
- [65] S. Aminikhahhahi and D. J. Cook, "A survey of methods for time series change point detection," *Knowl. Inf. Syst.*, vol. 51, no. 2, pp. 339–367, May 2017.
- [66] J. Bai and P. Perron, "Computation and analysis of multiple structural change models," *J. Appl. Econometrics*, vol. 18, no. 1, pp. 1–22, Jan. 2003.
- [67] S. Arlot, A. Célie, and Z. Harchaoui, "A kernel multiple change-point algorithm via model selection," *J. Mach. Learn. Res.*, vol. 20, no. 162, pp. 1–56, 2012.
- [68] P. Weber, P. Beldowski, A. Gadomski, K. Domino, P. Sionkowski, and D. Ledziński, "Statistical method for analysis of interactions between chosen protein and chondroitin sulfate in an aqueous environment," in *Perspectives in Dynamical Systems II—Numerical and Analytical Approaches*. Cham, Switzerland: Springer, 2022, pp. 697–714.
- [69] P. Sionkowski, N. Kruszewska, A. Kreitschitz, S. N. Gorb, and K. Domino, "Application of recurrence plot analysis to examine dynamics of biological molecules on the example of aggregation of seed mucilage components," *Entropy*, vol. 26, no. 5, p. 380, Apr. 2024.
- [70] C. Letellier, "Estimating the Shannon entropy: Recurrence plots versus symbolic dynamics," *Phys. Rev. Lett.*, vol. 96, no. 25, Jun. 2006, Art. no. 254102.
- [71] L. Cao, "Practical method for determining the minimum embedding dimension of a scalar time series," *Phys. D, Nonlinear Phenomena*, vol. 110, nos. 1–2, pp. 43–50, Dec. 1997.
- [72] Z. Ustrnul et al. (2024). *Bulletyn Monitoringu Klimatu Polski*. [Online]. Available: https://www.imgw.pl/sites/default/files/2024-05/imgw-pib_klimat_polski_2023_raport.pdf
- [73] K. Błażejczyk, R. Twardosz, and A. Kunert, "Zmienność warunków biotermicznych W Krakowie W XX wieku na tle wahań cyrkulacji atmosferycznej," in *Postępy W Badaniach Klimatycznych I Bioklimatycznych*, vol. 188. Warszawa, Poland: IGiPZ PAN, 2003, pp. 233–246.
- [74] D. Matuszko and S. Węglarczyk, "Long-term variability of the cloud amount and cloud genera and their relationship with circulation (Kraków, Poland)," *Int. J. Climatol.*, vol. 38, no. S1, pp. e1205–e1220, Apr. 2018.



Monika Okoniewska received the Ph.D. degree from the Institute of Geography and Spatial Organization, Polish Academy of Sciences, Warsaw, Poland, in 2011.

Since 2005, she has been employed at the Institute of Geography (currently the Faculty of Geographical Sciences), Kazimierz Wielki University(UKW), Bydgoszcz, Poland, and since 2012, she has held the position of an Assistant Professor. From 2016 to 2019, she was the Head of the Climatology Laboratory, Institute of Geography, UKW. Since 2024, she has been a member of the Research Team for the project titled "Extreme Weather Events Induced by Contemporary Climate Change and Their Impact on Humans and Their Functioning in the Natural Environment." In her work, in addition to educating students, she focuses on researching climate and bioclimate variability in Poland and Europe, the occurrence of extreme weather events and their impact on the human body (particularly heatwaves), the climate of urbanized areas, and the climatic and bioclimatic conditions for tourism and recreation.



Piotr Sionkowski received the M.Sc. degree in applied computer science from Warsaw University of Technology, Warsaw, Poland, in 2020.

He was a practitioner with over 12 years of industry experience, having worked for major technology (Akamai Technologies, Kraków, Poland; Nokia, IBM, Wrocław) and Fortune 500 companies (UBS, Kraków, and GSK, Poznań, Poland) in roles ranging from research and development and software and systems engineering to a focus on cybersecurity, which he transitioned to in 2021. Since 2022, he has

been collaborating with the Institute of Theoretical and Applied Informatics, Polish Academy of Sciences, Gliwice, Poland, where his research focuses on time series analysis, particularly using recurrence plots. In 2024, he began his role as the Principal Security Engineer of Akamai Technologies, Kraków.



Natalia Kruszewska received the master's degree in technical physics from the University of Technology and Agriculture, Bydgoszcz, Poland, in 2005, and the Ph.D. degree in physics from Silesian University, Katowice, Poland, in 2010.

She is currently an Assistant Professor at the Department of Physics, Bydgoszcz University of Science and Technology, Bydgoszcz, part of the Faculty of Chemical Technology and Engineering. She specializes in statistical and computer physics, thermodynamics, soft-matter theory, and the properties of complex networks. Her research focuses on applying computer models to study and analyze nonequilibrium thermodynamic processes, especially in biophysical contexts.



Krzysztof Błażejczyk is a Geographer-Climatologist Professor Emeritus. He is a Professor Emeritus at the Institute of Geography and Spatial Organization, Polish Academy of Sciences, Warsaw, Poland, and the University of Warsaw, Warsaw. He worked in many international teams coping with problems of urban heat islands, climate-related mortality in Europe, and the relation between solar radiation and circadian rhythm in humans. Together with experts from 18 European countries, he developed the universal thermal

climate index (UTCI). He is an expert in European Research Agency. His research concentrates on human bioclimatology (the influence of various climate features on the functioning of the human organism as well as on morbidity and mortality) and the climate of urban, recreational, and health resort areas. He carried out research dealing with the personal perception of climate and how climate impacts social and economic processes.



Krzysztof Domino received the M.Sc. degree in physics from Jagiellonian University, Kraków, Poland, in 2006, and the Ph.D. degree in physics from the Institute of Physics, Silesian University, Katowice, Poland, in 2015.

Due to experience in practice (almost eight years of work in industry) as well as science (concerning statistical analysis of data non-Gaussian distributions and knowledge of quantum physics), he was employed in 2015 by the Institute of Theoretical and Applied Informatics, Polish Academy of Sciences (IITiS), Gliwice, Poland, in particular as a Research Assistant, an Assistant Professor, and, since March 2020, as an Associate Professor. Since 2025, he has been the Leader of the Computer Vision Systems Group therein. He has been involved in many applied projects, as well as basic research projects, as a post-doctor, an expert, a manager, or a leader. His research concerns data analysis and optimization, both using classical as well as quantum approaches. His scientific career concerns combining fundamental research (physics, statistics, computer science, and quantum computing) with practical research and development.